Pre-perimetric Open Angle Glaucoma with Young Age of Onset: Natural Clinical Course and Risk Factors for Progression

EUNOO BAK, YONG WOO KIM, AHNUL HA, YOUNG KOOK KIM, KI HO PARK, AND JIN WOOK JEOUNG

• PURPOSE: To investigate the natural clinical course of more than 5 years and the risk factors of progression in patients with pre-perimetric open angle glaucoma (OAG) of "young age of onset (under age 40)" without treatment.

• DESIGN: Retrospective observational case series.

• METHODS: Optic disc photography, red-free retinal nerve fiber layer (RNFL) photography, optical coherence tomography, and visual field (VF) examinations were performed every 6 months. Glaucoma progression was defined as structural or functional deterioration. A linear mixed-effects model was used to estimate the rate of structural and functional changes. Kaplan-Meier survival analysis and log-rank testing were used to compare survival experiences, and Cox proportional hazards modeling was performed to identify risk factors for glaucoma progression.

• RESULTS: Of the 98 eyes of 98 patients (mean age, 30.6 years old), glaucoma progression was detected in 42 eyes (42.9%). The rate of average RNFL thickness thinning was −0.46 ± 0.50 μm/y, and the mean deviation (MD) change was −0.03 ± 0.13 dB/y. The glaucoma progression probability at 5 years was 39% by structural criteria and 5% by functional criteria. Older age at diagnosis ($P = .004$), presence of temporal raphe sign (horizontal straight line on macular ganglion cell-inner plexiform layer thickness map) ($P = .011$), lamina pore visibility ($P = .034$), and greater pattern standard deviation ($P = .005$) were significant factors for glaucoma progression.

• CONCLUSIONS: In untreated pre-perimetric OAG patients with a "young age of onset" condition, the estimated MD slope for the disease course of more than 5 years was −0.03 dB/y, and the average RNFL thinning rate was −0.46 μm/y. The predictors for progression were structural parameters of temporal raphe sign, lamina pore visibility, and functional parameter of pattern standard deviation. (Am J Ophthalmol 2020;216: 121–131. © 2020 Elsevier Inc. All rights reserved.)

THE RECENT AVAILABILITY OF ADVANCED TECHNOLOGY in diagnostic tests and improved strategies have facilitated earlier and more accurate detection of glaucomatous changes, even at the pre-perimetric stage.[1–3] Pre-perimetric open angle glaucoma (OAG) is characterized by the presence of glaucomatous optic disc (eg, neuroretinal rim thinning, notching, excavation) and damage in the retinal nerve fiber layer (RNFL), with normal visual field (VF) on standard automated perimetry (SAP).[3] According to previous studies, the factors associated with glaucoma progression are optic disc hemorrhage,[3–6] higher mean intraocular pressure (IOP),[3,6] fluctuation of IOP,[5] greater vertical cup-to-disc ratio,[5] and greater pattern standard deviation (PSD).[4] However, the treatment strategy for pre-perimetric OAG has not been well established.

The proportion of young adults in the glaucoma population is growing.[7,8] It has been previously reported that patients with myopic glaucoma are significantly younger than nonmyopic glaucoma patients.[9,10] Also, in a small cohort of 16 young (average, 38.9 years old) Chinese-American males with a diagnosis of glaucoma or suspected of having glaucoma, stable ocular findings were associated with myopia.[11] However, importantly, young patients have a longer life expectancy with the possibility of increased risk of end-of-life visual disabilities. Under this circumstance, knowledge of the natural course and risk of the disease progression, which presently is lacking, are essential.

Accordingly, the aim of this study was to investigate the over-5-year natural clinical course of pre-perimetric OAG of young age of onset (under age 40) without treatment. Additionally, the risk factors associated with structural and/or functional progression in these patients was evaluated.

SUBJECTS AND METHODS

THE PRESENT LONGITUDINAL RETROSPECTIVE STUDY included subjects from an ongoing study of a pre-

AJO.com Supplemental Material available at AJO.com.
Accepted for publication Mar 18, 2020.

From the Department of Ophthalmology (E.B., Y.W.K., A.H., Y.K.K., K.H.P., J.W.J.), Seoul National University College of Medicine, Seoul, Korea; and the Department of Ophthalmology (E.B., Y.W.K., A.H., Y.K.K., K.H.P., J.W.J.), Seoul National University Hospital, Seoul, Korea.

Inquiries to: Jin Wook Jeoung, Department of Ophthalmology, Seoul National University Hospital, Seoul National University College of Medicine, 101 Daehak-ro, Jongno-gu, Seoul 03080, Korea; e-mail: neuroprotect@gmail.com

0002-9394/$36.00
https://doi.org/10.1016/j.ajo.2020.03.026

perimetric OAG cohort at the Glaucoma Clinic of Seoul National University Hospital, examined between June 2008 and July 2015. The study protocol was approved by the Institutional Review Board of Seoul National University Hospital, and the study conduct adhered to the tenets of the Declaration of Helsinki.

The inclusion criteria were as follows: 1) young age at onset, under the age of 40, adults with pre-perimetric OAG; 2) a minimum of 5 years' follow-up without treatment; and 3) attendance at follow-up visits every 6 months. Additionally, the patients had a best corrected visual acuity better than 20/40, a spherical equivalent within ±8.0 D, good quality results of stereo optic disc photography, red-free results of retinal nerve fiber layer (RNFL) photographs, optical coherence tomography (OCT) images, and reliable VF test results (fixation loss <20%, false positive errors <15%, and false negative errors <15%). When both eyes met all eligibility criteria, 1 eye was randomly selected as the study eye.

Pre-perimetric OAG was defined as the presence of glaucomatous optic nerve damage (eg, focal notching, rim thinning), RNFL defect, open angle confirmed by gonioscopy, and the absence of definite glaucomatous VF defect in SAP at 3 initial consecutive VF examinations. Glaucomatous VF defect was defined as either 3 or more abnormal points with a P value of <.05, of which at least 1 point had a pattern standard deviation (PSD) of $P < .01$; or a PSD of $P < .05$; or glaucoma hemifield test values outside the normal limits. The age of onset of pre-perimetric OAG was considered the age at which the OAG was first diagnosed. During the initial examination of newly diagnosed pre-perimetric OAG, the possible clinical course of glaucoma was explained to all patients. The clinicians and patients also discussed whether to use IOP-lowering treatments. Patients agreed to undergo observation without IOP-lowering treatment unless a VF defect was identified. Patients who refused medication, despite having been informed of a new glaucomatous VF defect, were also observed without IOP-lowering treatment.

Patients were excluded for any of the following reasons: history of primary or secondary congenital glaucoma; history of primary or secondary juvenile glaucoma; secondary (eg, uveitic) glaucoma; , history of intraocular surgery or laser treatment (other than corneal refractive surgery); any systemic or ocular pathology known to affect the optic disc, RNFL, or VF (eg, retinal vascular occlusive disease, hypertensive retinopathy, ocular infection, trauma); segmentation failure in OCT scans of the RNFL or ganglion cell-inner plexiform layer (GCIPL) in the optic disc or macular cube on 4 or more consecutive visits; total follow-up duration of less than 5 years after exclusion of OCT scans[12]; or low reliability of VF index (fixation loss >20%, false positive errors>15%, false negative errors >15%). The first VF available from each participant was excluded due to the possibility of a learning effect.[13] The VF tests were reviewed for the presence of artifacts including fatigue or learning effects, inattention, inappropriate fixation, or eyelid or rim artifacts. Tests results with such artifacts were excluded from the analyses.

All subjects underwent complete ophthalmic examinations including a review of medical history; visual acuity; Goldmann applanation tonometry; refraction (KR-890; Topcon, Tokyo, Japan); slit-lamp biomicroscopy; gonioscopy; dilated fundus examination; digital color stereo optic disc photography; red-free RNFL photography (TRC-50IX; Topcon); and SAP (Humphrey 30-2 SITA-standard visual field; Carl Zeiss Meditec, Dublin, California). In addition, central corneal thickness (Pocket II Pachymeter Echograph; Quantel Medical, Clermont-Ferrand, France) and axial length (AXIS-II ultrasonic biometer; Quantel Medical SA, Bozeman, Montana) were measured. The patients attended regular follow-up visits at 6-month intervals, at which time they underwent clinical examinations, optic disc photography, red-free RNFL photography, and SAP.

A calibrated Goldmann applanation tonometer was used to measure IOP at the baseline and follow-up visits during office hours (8:30 AM to 5:30 PM) with the patient in a sitting position under topical anesthesia. Baseline IOP was defined as the mean of 2 values obtained at 2 consecutive visits.[14] The mean follow-up IOP was calculated as the average of all IOPs for all visits without IOP-lowering treatment. Fluctuation of IOP was defined based on the standard deviation of those mean values.[15]

• **EVALUATION OF OPTIC DISC IMAGES:** All optic disc and RNFL photographs were obtained after dilation of the patient's pupil. Images were taken by a single experienced examiner with a simultaneous camera. After a scanning process, images were saved in a 1,600- × 1,216-pixel digital imaging format and stored in the picture-archiving communication system of Seoul National University Hospital. The stereoscopic disc photograph was centered on the optic disc. By photographically focusing on the lamina cribrosa (LC), the clear visibility of lamina pores was assessed. The presence of lamina pore visibility was assessed by 2 glaucoma specialists (E.B., Y.W.K.). In cases of disagreement, a third glaucoma specialist (J.W.J.) confirmed the presence after discussion. A disc hemorrhage was considered a splinter- or flame-shaped hemorrhage adjacent to the optic disc or parapapillary area and extending to the border of the optic disc. β-Zone parapapillary atrophy (PPA) was defined as an area adjacent to the disc margin with notable atrophy of the retinal pigment epithelium, visible sclera, and visible large choroidal vessels.

Measurements were taken by using ImageJ version 1.52 software (National Institutes of Health, Bethesda, Maryland). Images were evaluated by 2 glaucoma specialists (E.B., Y.W.K.) who were masked to all patients' clinical information. The representative value was considered the average of the values measured by the 2 specialists. The extent of disc tilt was defined as the longest-to-shortest

diameter ratio of the optic disc. The area was delineated by using a mouse-driven cursor to trace the PPA and disc margins directly onto the disc photograph image. The structures for quantification were outlined on the inside edge in order that the trace thickness could be incorporated into the total delineated area. Instead of the β-zone PPA area itself, the β-zone PPA-to-disc area ratio was used to minimize the effects of photographic magnification error.

• **SD-OCT IMAGING:** Cirrus HD-OCT version 9.5 software (Carl Zeiss Meditec) was used to acquire RNFL and macular GCIPL measurements. Measurements were taken by a single experienced examiner after mydriasis of the patients' eyes. RNFL thicknesses were measured from an optic disc cube scan (200 × 200 pixels) generating an RNFL thickness map of the parapapillary region (6 × 6 mm^2). Parameters included peripapillary global average RNFL thickness; 4-quadrant thickness; thickness at 12 O'clock; optic nerve head (ONH) parameters at the rim area and disc area; average cup-to-disc ratio; vertical cup-to-disc ratio; and cup volume.

GCIPL thicknesses were measured from a macular cube scan (200 × 200 pixels) generating a GCIPL thickness map in an elliptical annulus (inner vertical and horizontal axes of 1.0 mm and 1.2 mm, respectively; and outer vertical and horizontal axes of 4.0 mm and 4.8 mm, respectively) centered at the fovea. The average, minimum, and sectoral (superonasal, superior, superotemporal, inferotemporal, inferior, and inferonasal) measurements were obtained. The temporal raphe sign was determined as a horizontal straight line located in the temporal elliptical area (longer than one-half of the length between the inner and outer annulus).[16]

Satisfactory OCT quality was defined as 1) a well-focused image, 2) the presence of a centered circular ring around the optic disc, and 3) a signal strength ≥6.[17] OCT scans with motion artifacts, poor centration, or missing data were discarded, and eyes were rescanned on the same day. If only the optic disc or macular cube scan of an eye met the requirement for image quality, both scans were removed from the longitudinal analysis.

• **DETERMINATION OF GLAUCOMA PROGRESSION:** Structural changes on disc and/or RNFL photographs and functional changes on SAP were assessed to determine the patient's progression status. The first time that structural or functional progression was detected was considered the "progression endpoint."

Structural progression was defined as progression of the optic disc and/or RNFL defect change in 2 consecutive examinations within an interval of 6 months. Progressive optic disc changes included focal, diffuse narrowing or notching of the neuroretinal rim; increased cup-to-disc ratio; or changes in the adjacent vasculature, as determined by comparison of serial disc photographs.[3,5] The definition of change was not based on the presence of disc hemorrhage, deepening of the cup, color change, or changes resulting from differences in focus. Progressive RNFL defect changes were determined based on increased width or depth of an existing defect or the appearance of a new defect. All photographs were evaluated, and changes were confirmed by 2 experienced glaucoma specialists (E.B., Y.W.K.), both of whom were masked to all patients' information and other findings, independently. Each patient was classified as a structural nonprogressor or progressor based on interpretation of disc and RNFL photographs. Disagreements were adjudicated by discussion with a third glaucoma specialist (J.W.J.).

Functional progression observed on VF test results was defined in reference to previous studies.[17–20] Progression of VF was evaluated by 2 methods, the "event-based" analysis and the "trend-based" analysis. Event-based analysis detects whether significant deterioration has occurred, whereas trend-based analysis calculates the rate of progression. In the present event-based analysis, the guided progression analysis application of the Humphrey field analyzer with guided progression analysis software was used, and significant VF progression was diagnosed if the guided progression analysis result indicated "likely progression." "Likely progression" manifests as 3 or more test point locations that are anywhere in the field and not necessarily contiguous and that show significant deterioration in 3 consecutive tests.[18,21] In the present trend-based analysis, linear regression analysis was used to calculate the rate of progression based on the change in mean deviation (MD) over time. One glaucoma specialist (A.H.), masked to the patients' clinical information, reviewed the serial VF test results for artifacts by double-checking.

• **STATISTICAL ANALYSIS:** The clinical characteristics of the continuous variables were compared by using the Student *t*-test, and the categorical variables were compared by using chi-squared tests. A linear mixed-effects model was used to estimate the rates of global and sectoral RNFL, GCIPL thickness, and VF parameter change. For validation of the interobserver agreement on glaucoma progression, the presence of lamina pore visibility, measurements of the extent of disc tilt and β-zone-to-disc-area ratio, and Kappa (κ) statistics were assessed. The strength of agreement was categorized according to classification by Landis and Koch[22]: 0 = poor; 0-0.20 = slight; 0.21-0.40 = fair; 0.41-0.60 = moderate; 0.61-0.80 = substantial; and 0.81-1.00 = almost perfect. Univariate and multivariate Cox proportional hazards regression models were used to identify factors associated with structural and functional progression. The variables with significance at $P < .10$ in the univariate model were included in the subsequent multivariate model. The final multivariate model was developed by means of backward elimination, and the adjusted hazard ratio (HR) with a 95% confidence interval (CI) was calculated. Kaplan-Meier survival analysis based on structural and functional deterioration was

TABLE 1. Demographics and Clinical Characteristics of Young Preperimetric Open Angle Glaucoma Patients

	Nonprogressing Group (n = 56)	Progressing Group (n = 42)	*P* Value
Demographic variables			
Mean ± SD age at diagnosis, y	30.1 ± 6.4	31.3 ± 5.7	.84[a]
Male	28 (53.8%)	22 (47.8%)	.93[b]
Mean ± SD spherical equivalence, D	−5.04 ± 2.75	−5.02 ± 2.66	.94[a]
Mean ± SD axial length, mm	25.44 ± 1.72	25.53 ± 1.18	.40[a]
Mean ± SD central corneal thickness, μm	547.1 ± 42.1	543.4 ± 48.4	.82[a]
Mean ± SD baseline IOP, mm Hg	15.0 ± 3.4	14.5 ± 3.0	.84[a]
Mean ± SD IOP, mm Hg	14.5 ± 2.5	13.9 ± 2.3	.82[a]
Mean ± SD IOP fluctuation, mm Hg	1.7 ± 0.7	1.5 ± 0.6	.82[a]
Optic disc hemorrhage	0 (0.0%)	2 (4.7%)	.10[b]
Family history of glaucoma	8 (15.4%)	3 (6.5%)	.87[b]
Hypertension	3 (5.8%)	2 (4.3%)	.93[b]
Diabetes mellitus	0 (0.0%)	0 (0.0%)	>.99[b]
Structural Parameters			
Temporal raphe sign	8 (15.4%)	16 (34.8%)	.06[b]
Visible lamina pore	27 (51.9%)	31 (67.4%)	.06[b]
Mean ± SD tilt ratio	1.19 ± 0.17	1.22 ± 0.15	.25[a]
Mean ± SD PPA-to-disc area ratio	0.52 ± 0.50	0.50 ± 0.45	.74[a]
Mean ± SD Vertical cup/disc ratio	0.65 ± 0.10	0.66 ± 0.09	.49[a]
Mean ± SD baseline RNFL thickness, μm	85.8 ± 7.7	85.5 ± 8.7	.93[a]
Mean ± SD baseline GCIPL thickness, μm	73.1 ± 8.6	74.3 ± 6.4	.87[a]
Mean ± SD functional parameters			
Baseline MD, dB	−0.30 ± 1.32	−0.24 ± 1.22	.82[a]
Baseline PSD, dB	1.81 ± 0.56	2.09 ± 0.66	.06[a]

Values are mean ± SD and n (%). *P* values were adjusted using the Benjamini-Hochberg method to compensate for multiple comparison.
D = diopters; GCIPL = ganglion cell-inner plexiform layer; IOP = intraocular pressure; MD = mean deviation; dB = decibels; PPA = parapapillary atrophy; PSD = pattern standard deviation; RNFL = retinal nerve fiber layer;
[a]Student *t*-test.
[b]Chi-square test.

evaluated, and the cumulative probability of structural progression between progressors and nonprogressors was stratified by the significantly associated factors. Statistical analyses were performed using statistical software (SPSS version 22.0; SPSS Inc, Chicago, Illinois) and R version 3.5.3 software (R Foundation, Vienna, Austria)). Statistical significance was set at a *P* value of $< .05$, and the false discovery rate was controlled using the Benjamini-Hochberg method.

RESULTS

A TOTAL OF 133 YOUNG-AGE-ONSET (UNDER AGE 40) PREperimetric OAG patients without treatment were followed for more than 5 years, between 2008 and 2015. Among them, 12 patients with poor quality stereo disc photographs and/or red-free RNFL photographs; 2 patients with a follow-up duration less than 5 years after exclusion of poor quality OCT scans; 4 patients with segmentation failure of OCT scans on 4 or more visits; and 17 patients with unreliable VF results were excluded from the analyses. Ultimately, 98 eyes of 98 patients were included for analysis (mean follow-up duration, 5.8 ± 1.7 years; mean age at diagnosis, 30.6 years old [range, 20-39 years old]; and baseline IOP, 14.8 ± 3.2 mm Hg).

• **DEMOGRAPHIC AND CLINICAL CHARACTERISTICS OF PROGRESSORS AND NONPROGRESSORS:** The patients' demographic and baseline clinical characteristics are summarized in Table 1. Of 98 patients, 42 (42.9%) presented with glaucoma progression and were classified as progressors, and 56 patients (57.1%) without progression were classified as nonprogressors. All 42 progressors exhibited structural progression (optic disc and/or RNFL deterioration), and 5 of them showed both structural and functional progression (VF deterioration). The interobserver agreement on structural progression was almost perfect ($\kappa = 0.86$; 95% CI: 0.82-0.91). Seven cases had observer disagreement on

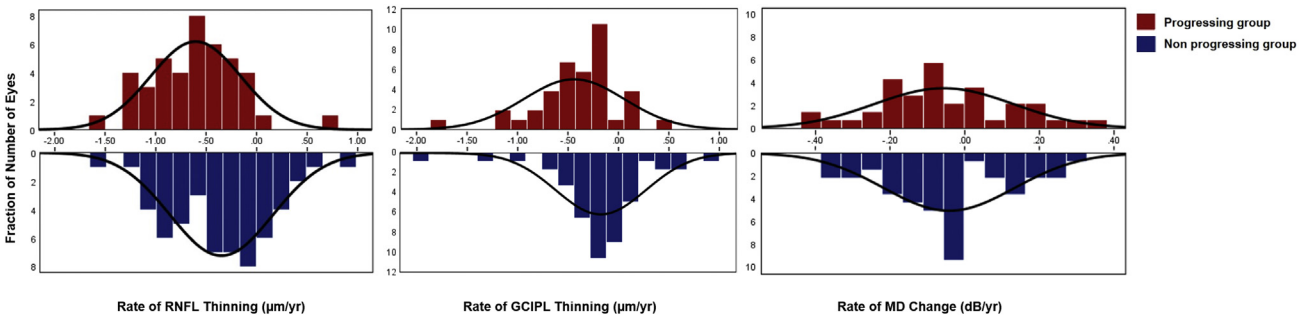

FIGURE 1. Distribution of rates of change for average retinal nerve fiber layer (RNFL) and ganglion cell-inner plexiform layer (GCIPL) thickness and mean deviation (MD) of visual field. Histograms comparing rates of change for RNFL thickness (left), GCIPL thickness (middle), and MD of visual field (right) between eyes with structural progression (red) and nonprogression (blue).

structural evaluation, and no case had disagreement on functional evaluation. For the 7 cases of disagreement, the third adjudicator classified 3 progressors and 4 nonprogressors. No significant differences of the baseline characteristics were found between progressors and nonprogressors. The inter-observer values were almost perfect for lamina pore visibility ($\kappa = 0.98$; 95% CI: 0.97-0.99), tilt ratio ($\kappa = 0.91$; 95% CI: 0.84-0.95), and PPA-to-disc area ratio ($\kappa = 0.90$; 95% CI: 0.82-0.94).

• **RATE OF PROGRESSION:** Analysis of the rates of change of the structural and functional parameters are shown in Figure 1 and Table 2. During the follow-up period (5.8 ± 1.7 years), the overall average RNFL thickness slope was −0.46 ± 0.50 μm/y (95% CI, −0.56 to −0.36), the average GCIPL thickness slope was −0.29 ± 0.83 μm/y (95% CI, −0.45 to −0.12), and the mean MD change was −0.03 ± 0.13 dB/y (95% CI, −0.06 to −0.01). The average RNFL thickness slope was greater for progressors than for nonprogressors (−0.60 ± 0.45 vs. −0.35 ± 0.51 μm/y, respectively; adjusted $P = .007$), and the rate was fastest in the inferior quadrant (−1.27 ± 1.06 vs. −0.71 ± 0.83 μm/y, respectively; adjusted $P = .006$). The average GCIPL thickness slope also was greater for progressors than for nonprogressors (−0.58 ± 0.94 vs. −0.07 ± 0.67 μm/y, respectively; adjusted $P < .001$). The MD rate did not show statistical difference (−0.06 ± 0.12 dB/y vs. −0.02 ± 0.13, respectively; adjusted $P = .33$). The rates of RNFL thinning for clock-hour sectoral RNFL thickness are compared in Supplemental Table 1, and the baseline-to-final changes of the structural and functional parameters are listed in Supplemental Tables 2 and 3. Representative cases of structural progression (Figure 2) and nonprogression (Figure 3) followed over the course of 7 years are shown.

• **RISK FACTORS FOR GLAUCOMA PROGRESSION:** The baseline factors were analyzed by a univariate Cox proportional hazard model. Older age at presentation (HR = 1.081; $P = .004$), presence of temporal raphe sign (HR = 2.277; $P = .011$), lamina pore visibility (HR = 2.134; $P = .034$), and greater PSD (HR = 1.944; $P = .005$) significantly contributed to glaucoma progression (Table 3).

In Kaplan-Meier survival analysis, the glaucoma progression probability at 5 years was 39% (95% CI, 29-49) according to the structural criteria, and 5% according to the functional criteria. Patients with temporal raphe sign showed a significantly greater cumulative probability of glaucoma progression ($P = .028$) (Figure 4A). In addition, patients with the visibility of lamina pore had a greater cumulative probability of glaucoma progression ($P = .036$) (Figure 4B).

DISCUSSION

THIS STUDY INVESTIGATED THE NATURAL CLINICAL course of young-age-onset (age less than 40 years old) pre-perimetric OAG patients without treatment and characterized the progression rate and risk factors of glaucoma progression in these patients. After more than 5 years of follow-up, 42.9% of patients showed structural or functional progression with a total mean RNFL thickness change of −0.46 ± 0.50 μm/y and a MD change of −0.03 ± 0.15 dB/y. Older age at diagnosis, presence of temporal raphe sign, lamina pore visibility, and greater PSD were factors associated with glaucoma progression.

In this study, the proportion of glaucoma progression was low compared with that in previous reports of onset in old age (over 40 years old) treated pre-perimetric OAG patients (42.9 vs. 56.7%, respectively).[3] A relatively slow global RNFL thinning rate was observed in this study (−0.46 vs. −0.34 to −2.02 μm/y, respectively).[17,23,24] The phenomenon can be explained by the effect of age-associated change and the presence of myopia. In previous studies, the average rate of OCT-derived measurements differed by age-related changes and was significantly higher in subjects older than 41 years.[25–27] Because the present study enrolled patients under 40 years old, previous studies without any age limitation (average age 53.1-64.5) may have had a faster

TABLE 2. Rates of Change for Structural and Functional Parameters

	Total	Nonprogressing Group (n = 52)	Progressing Group (n = 46)	*P* Value
Mean ± SD RNFL thickness parameters (range)				
Average, μm/y	−0.46 ± 0.50 (−0.56 to −0.36)	−0.35 ± 0.51 (−0.49 to −0.21)	−0.60 ± 0.45 (−0.74 to −0.46)	.007[a]
Superior, μm/y	−0.47 ± 0.63 (−0.60 to −0.35)	−0.42 ± 0.63 (−0.59 to −0.25)	−0.55 ± 0.52 (−0.74 to −0.35)	.22
Inferior, μm/y	−0.95 ± 1.04 (−1.16 to −0.74)	−0.71 ± 0.83 (−0.10 to −0.43)	−1.27 ± 1.06 (−1.57 to −0.98)	.006[a]
GCIPL thickness parameters (range)				
Average, μm/y	−0.29 ± 0.83 (−0.45 to −0.12)	−0.07 ± 0.66 (−0.24 to −0.11)	−0.58 ± 0.94 (−0.87 to −0.29)	<.001[a]
Superior, μm/y	−0.04 ± 0.25 (−0.09 to −0.01)	−0.01 ± 0.23 (−0.04 to 0.01)	−0.08 ± 0.50 (−0.19 to 0.02)	.32
Inferior, μm/y	−0.34 ± 0.82 (−0.50 to −0.17)	−0.13 ± 0.60 (−0.03 to 0.08)	−0.62 ± 0.50 (−0.87 to −0.37)	<.001[a]
Mean ± SD functional parameters (range)				
MD, dB/y	−0.03 ± 0.13 (−0.06 to −0.01)	−0.02 ± 0.13 (−0.05 to 0.01)	−0.06 ± 0.12 (−0.09 to −0.02)	.33

Values are mean ± SD. *P* values were adjusted by using the Benjamini-Hochberg method to compensate for multiple comparison.
GCIPL = ganglion cell-inner plexiform layer; MD = mean deviation; RNFL = retinal nerve fiber layer;
[a]Significant *P* values, <.05.

structural rate than that in the present data (average, 30.6 years old).[17,23,24] Also, the average myopic degree was −5.03 D in this study. As previously reported, myopia may contribute as a protective factor for RNFL progression.[9] Further study results classified by myopic degree are promising. Moreover, the overall MD progression rate was slow in the present cohort of patients compared with that in studies of old-age patients (−0.03 vs. −0.09 to −0.39 dB/year).[3,4,6] These findings of structural and functional progression rates suggest that, in pre-perimetric OAG patients of young-age onset glaucoma, progression may occur less often and more slowly, even without treatment.

In the present pre-perimetric OAG cohort, relatively older age at onset was associated with glaucomatous progression. The reason for this is not yet clear; however, it may be explained in terms of the aspect of myopia with glaucomatous-like defects in younger subjects. Myopia is rapidly increasing in young populations,[28–30] and myopic glaucoma patients are significantly younger than nonmyopic glaucoma patients.[9,10] Although debate is ongoing,[31,32] previous studies have reported that myopia does not contribute to glaucoma progression and may even act as a protective factor.[9,11,33,34] Glaucomatous changes in young patients may be coincidental with myopic developmental changes such as increased axial length and optic disc tilt. However, as myopic changes are usually stable after adolescence,[35,36] by the time adulthood is reached, these glaucomatous-like defects may have stabilized at the initial ophthalmic examination. Further studies will be needed to prove this hypothesis.

The laminar dot sign, a classical ONH sign of glaucoma, is visible as gray pores of the ONH representing the exposed underlying LC tissue.[37] Load-related deformation of the LC is posited as a cause of glaucoma.[38,39] The presence of visible lamina pores predicting glaucoma progression in this study can be explained as follows. Once the connective tissues of the LC mechanically fail, the lamina pore becomes visible, and the remaining adjacent healthy LC suffers from strain.[40] This can cause damage to the axons passing through the LC, which leads to progressive glaucomatous change.

In the present study, significant thinning of GCIPL thickness was detected in the progressor group (average and inferior area, both $P < .001$ respectively), and the temporal raphe sign was associated with glaucoma progression. The temporal raphe sign is a horizontal straight line on the macular GCIPL map showing a step-like configuration near the temporal raphe.[16] It is useful in glaucoma diagnosis, especially for early structural changes and myopic eyes[16,41–43] and also is predictive of VF progression.[12,44] We can assume that the presence of the temporal raphe sign is a reflection of early glaucomatous structural loss in pre-perimetric glaucoma, which eventually leads to further glaucoma progression.

PSD is the measurement of localized VF defect that best quantifies progression of glaucoma in early stages with monotonic increment.[45] Greater PSD (more damage to the VF) is predictive of an increased probability of progression from ocular hypertension to POAG,[46–48] and development of glaucomatous VFD in pre-perimetric OAG.[4] In this study, a greater PSD value was correlated with glaucoma progression, which fact indicated that early levels of VF damage at the pre-perimetric stage are risk factors for glaucoma progression.

The study has possible limitations. First, all patients enrolled were Koreans from a single center. East Asian populations show a high prevalence of myopia relative to other populations.[10] Moreover, ethnic difference may affect the progression rate of glaucoma.[49] These facts could

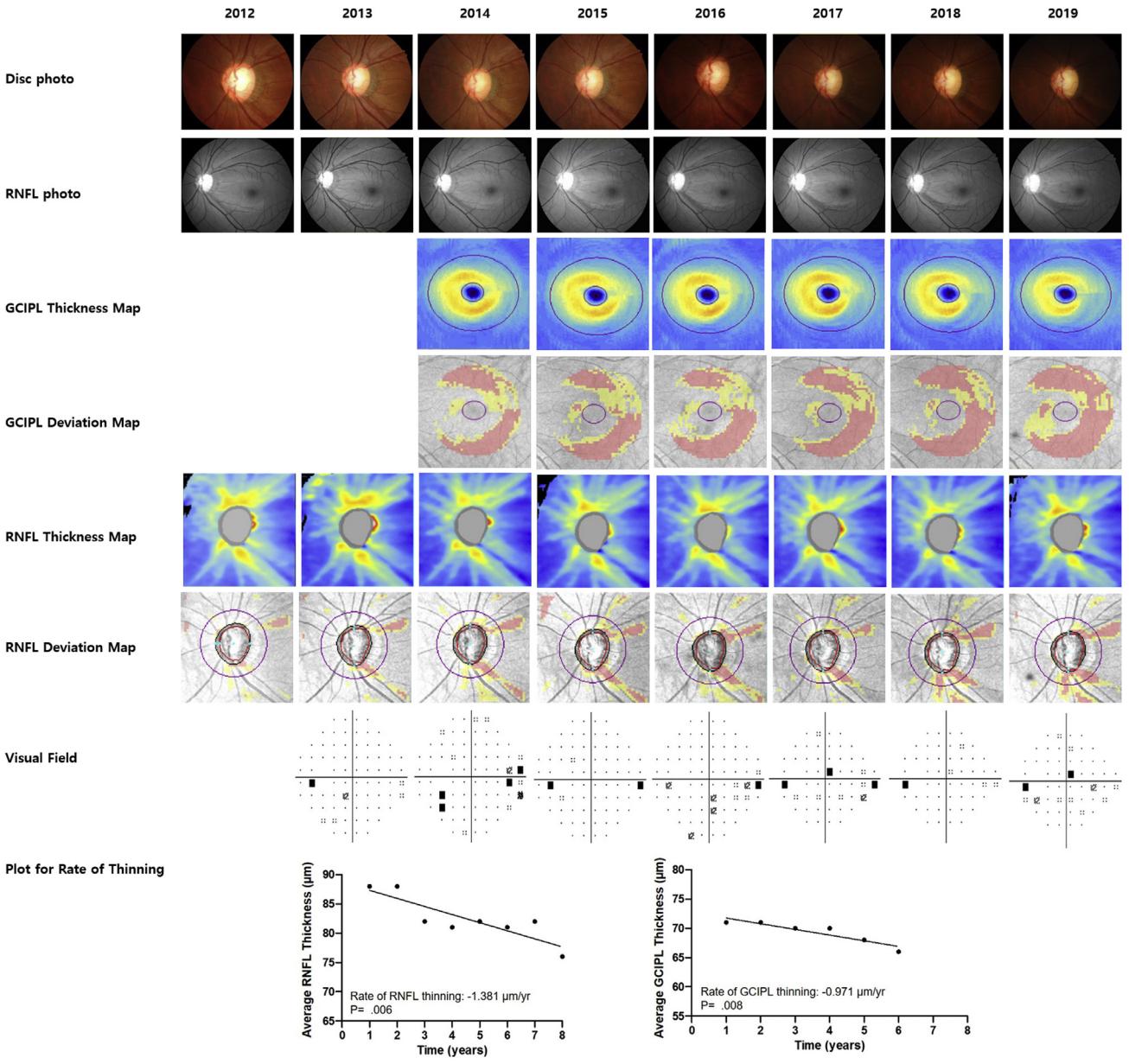

FIGURE 2. Representative case of structural progression. Left eye of 34-year-old female demonstrating progressive structural change during 7-year follow-up. Progressive inferior disc rim narrowing (first row) and corresponding retinal nerve fiber layer (RNFL) defect widening (second row) were observed. Progressive macular ganglion cell-inner plexiform layer (GCIPL) thinning is demonstrated in the serial illustration of GCIPL thickness (third row) and deviation map (fourth row). Progressive RNFL thinning is demonstrated in the serial illustration of RNFL thickness (Fifth row) and deviation map (sixth row). No significant progression was detected in the pattern deviation plot of visual field (seventh row). The global rates of RNFL and GCIPL thinning were −1.38 ± 0.33 µm/y (P = .006) and −0.97 ± 0.20 µm/y (P = .008), respectively (Last row).

have influenced our findings, in which case, they may not pertain to other ethnic groups. Second, diagnosis of preperimetric glaucoma can vary among clinicians because of the subjective nature of structural evaluation. However, this study included cases of definite glaucomatous optic neuropathy with distinct RNFL defect on the disc and RNFL photography, which differ from cases of ocular hypertension or glaucoma suspect without structural damage at baseline.[50,51] Also, progression of structural progression may differ among studies. It is defined here as the progression of the optic disc and/or RNFL defect change. Although serial RNFL examinations by photography results are known to be sensitive in detecting glaucoma progression,[52] it is often difficult to clearly determine the borders of diffuse RNFL atrophy, which may lead to challenges in identification of RNFL defect changes. Therefore,

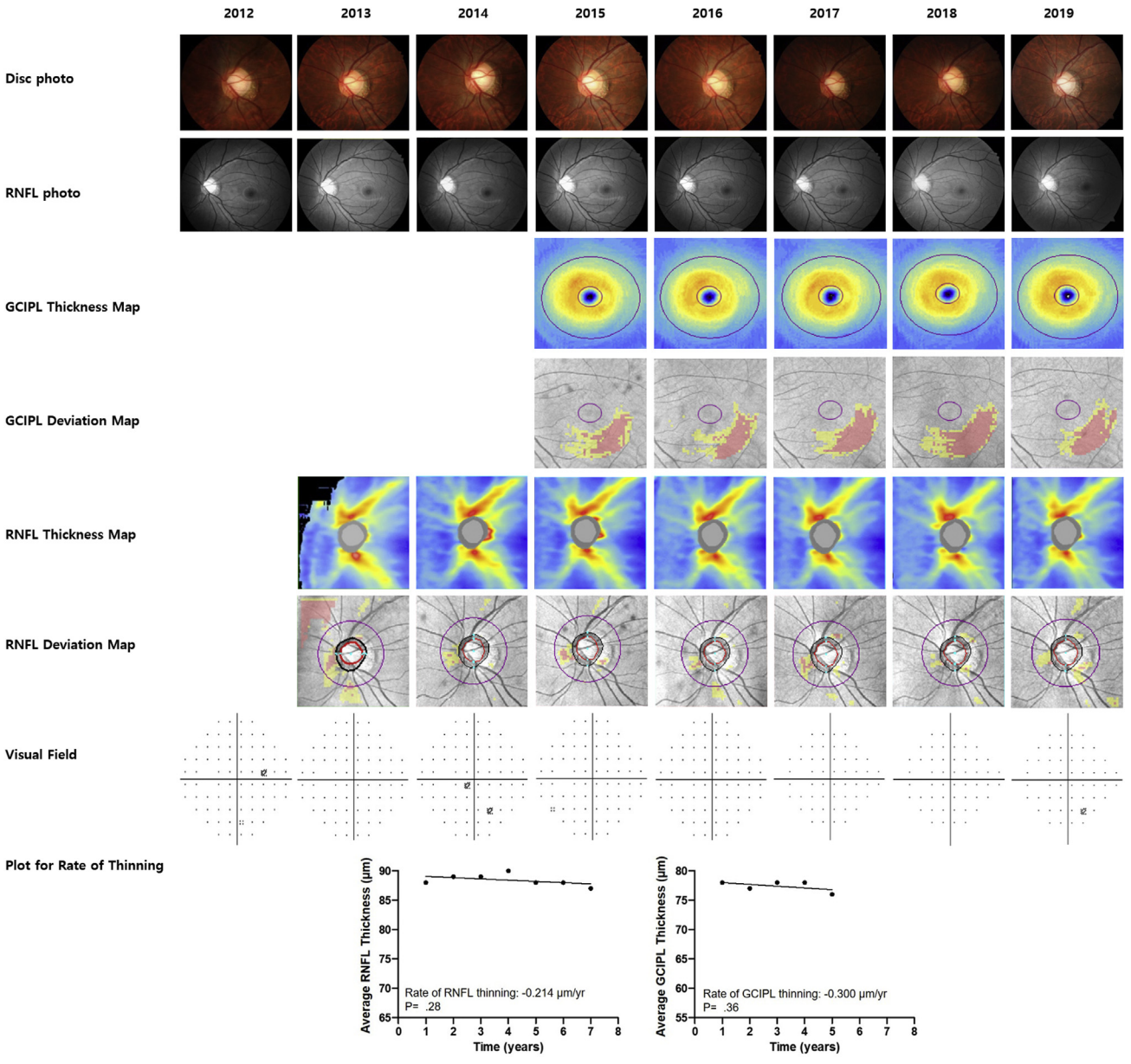

FIGURE 3. Representative case of nonprogressing eye. Left eye of 27-year-old male demonstrating no significant structural progression during 7-year follow-up. The stereo-optic disc photography (First row), red-free retinal nerve fiber layer (RNFL) photography (second row), RNFL thickness and deviation map (third and fourth row), ganglion cell-inner plexiform layer (GCIPL) thickness and deviation map (fifth and sixth row), and visual field (seventh row) were stationary. The global rates of RNFL and GCIPL thinning were −0.21 ± 0.17 µm/y ($P = .28$) and −0.30 ± 0.28 µm/y ($P = .36$), respectively (last row).

evaluating the progression of optic disc and/or RNFL defect would be necessary in order to define the structural progression of glaucoma.[53] Third, unlike previous studies, we could not statistically prove the presence of disc hemorrhage as a factor associated with glaucoma progression.[3–6] This outcome seems to be based on the fact that all patients with disc hemorrhage in this study also presented with glaucoma progression, but the number was relatively small (only 2 patients), not enough to show statistical significance. Moreover, disc hemorrhage occurs frequently in older age.[54,55] The incidence reported from a nationwide cross-sectional survey of a Korean population of glaucoma patients was extremely low (ie, 0%) in the group younger than 40 years old, which contrasted with the greater occurrence found in the older age groups.[56] Fourth, this study assessed the PPA with the use of stereo photographs. Spectral-domain OCT would be a useful method for investigation of PPA morphology, which is warranted in further studies. Fifth, OCT-derived measurements were based on a different OCT device than those

TABLE 3. Cox Proportional Hazard Model for Structural or Functional Progression

Variables	Univariate Model		Multivariate Model	
	HR (95% CI)	*P* Value	HR (95% CI)	*P* Value
Continuous variables				
Age at diagnosis, per year	1.074 (1.017-1.133)	.09	1.081 (1.025-1.140)	.004[a]
Axial length, per mm	1.090 (0.879-1.352)	.43		
Central corneal thickness, per μm	1.000 (0.992-1.007)	.94		
Mean IOP, per mm Hg	1.017 (0.903-1.144)	.79		
IOP fluctuation, per mm Hg	0.812 (0.592-1.509)	.81		
History				
Male	1.060 (0.577-1.948)	.85		
History of disc hemorrhage	2.644 (0.632-11.054)	.18		
Family history of glaucoma	0.568 (0.176-1.828)	.34		
History of hypertension	1.182 (0.362-3.866)	.78		
Structural parameters				
Baseline temporal raphe sign	2.154 (1.150-4.036)	.017[a]	2.277 (1.211-4.280)	.011[a]
Baseline visible laminar pore	1.898 (0.950-3.793)	.07	2.134 (1.059-4.299)	.034[a]
Tilt ratio	2.226 (0.445-11.138)	.33		
PPA-to-disc area ratio	1.185 (0.626-2.244)	.60		
Vertical cup/disc ratio	1.538 (0.063-37.821)	.79		
Functional parameters				
Baseline MD, per dB	1.013 (0.796-1.288)	.92		
Baseline PSD, per dB	1.660 (1.137-2.425)	.009[a]	1.944 (1.219-3.102)	.005[a]

Factors with $P < .10$ in the univariate analysis were included in the multivariate analysis.

CI = confidence interval; dB = decibels; HR = hazard ratio; IOP = intraocular pressure; MD = mean deviation; PPA = parapapillary atrophy; PSD = pattern standard deviation.

[a]Significant values with $P < .05$.

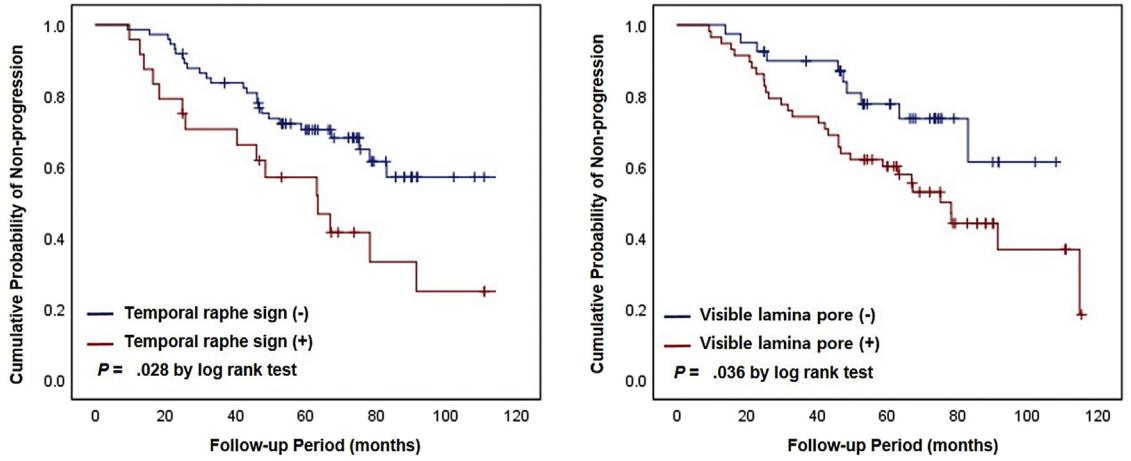

FIGURE 4. Kaplan-Meier survival analysis.

used in other studies.[23,24] Previous studies have revealed that the RNFL thickness values measured with different devices are not interchangeable.[57,58] Thus, the use of a different OCT device in the present study might have affected the rate of glaucoma progression.

In conclusion, the present study provided novel information on the natural clinical course of "young age of onset' pre-perimetric OAG patients without treatment. The progression rate was relatively slow, even without treatment: 39% indicated structural progression and only 5% VF progression during a period of 5 years. For prediction of glaucomatous progression, careful inspection of the structural parameters of temporal raphe sign, lamina pore visibility, and the functional parameter of PSD are needed.

CRediT AUTHORSHIP CONTRIBUTION STATEMENT

EUNOO BAK: DATA CURATION, FORMAL ANALYSIS, WRITING - original draft, Writing - review & editing. **Yong Woo Kim:** Data curation, Formal analysis, Writing - review & editing. **Ahnul Ha:** Data curation, Formal analysis. **Young Kook Kim:** Formal analysis, Data curation. **Ki Ho Park:** Formal analysis, Data curation. **Jin Wook Jeoung:** Conceptualization, Data curation, Formal analysis, Writing - review & editing.

ALL AUTHORS HAVE COMPLETED AND SUBMITTED THE ICMJE FORM FOR DISCLOSURE OF POTENTIAL CONFLICTS OF INTEREST and none were reported.

Funding/Support: No outside funding was received for this work.

Financial Disclosures: The authors have reported that they have no relationships relevant to the contents of this paper to disclose.

REFERENCES

1. Lisboa R, Paranhos A Jr, Weinreb RN, Zangwill LM, Leite MT, Medeiros FA. Comparison of different spectral domain OCT scanning protocols for diagnosing pre-perimetric glaucoma. *Invest Ophthalmol Vis Sci* 2013;54:3417–3425.
2. Tatham AJ, Weinreb RN, Medeiros FA. Strategies for improving early detection of glaucoma: the combined structure-function index. *Clin Ophthalmol* 2014;8:611–621.
3. Kim KE, Jeoung JW, Kim DM, Ahn SJ, Park KH, Kim SH. Long-term follow-up in pre-perimetric open-angle glaucoma: progression rates and associated factors. *Am J Ophthalmol* 2015;159:160–168.
4. Sawada A, Manabe Y, Yamamoto T, Nagata C. Long-term clinical course of normotensive pre-perimetric glaucoma. *Br J Ophthalmol* 2017;101:1649–1653.
5. Sakata R, Yoshitomi T, Iwase A, et al. Factors associated with progression of Japanese open-angle glaucoma with lower normal intraocular pressure. *Ophthalmology* 2019;126:1107–1116.
6. Jeong JH, Park KH, Jeoung JW, Kim DM. Pre-perimetric normal tension glaucoma study: long-term clinical course and effect of therapeutic lowering of intraocular pressure. *Acta Ophthalmol* 2014;92:e185–e193.
7. Marx-Gross S, Laubert-Reh D, Schneider A, et al. The prevalence of glaucoma in young people. *Dtsch Arztebl Int* 2017;114:204–210.
8. Vajaranant TS, Wu S, Torres M, Varma R. The changing face of primary open-angle glaucoma in the United States: demographic and geographic changes from 2011 to 2050. *Am J Ophthalmol* 2012;154:303–314.
9. Lee JY, Sung KR, Han S, Na JH. Effect of myopia on the progression of primary open-angle glaucoma. *Invest Ophthalmol Vis Sci* 2015;56:1775–1781.
10. Park HY, Lee K, Park CK. Optic disc torsion direction predicts the location of glaucomatous damage in normal-tension glaucoma patients with myopia. *Ophthalmology* 2012;119:1844–1851.
11. Doshi A, Kreidl KO, Lombardi L, Sakamoto DK, Singh K. Nonprogressive glaucomatous cupping and visual field abnormalities in young Chinese males. *Ophthalmology* 2007;114:472–479.
12. Hou HW, Lin C, Leung CK. Integrating macular ganglion cell inner plexiform layer and parapapillary retinal nerve fiber layer measurements to detect glaucoma progression. *Ophthalmology* 2018;125:822–831.
13. Racette L, Liebmann JM, Girkin CA, et al. African Descent and Glaucoma Evaluation Study (ADAGES): III. Ancestry differences in visual function in healthy eyes. *JAMA Ophthalmol* 2010;128:551–559.
14. Heijl A, Leske MC, Hyman L, Yang Z, Bengtsson B. Intraocular pressure reduction with a fixed treatment protocol in the Early Manifest Glaucoma Trial. *Acta Ophthalmol* 2011;89:749–754.
15. Caprioli J, Coleman AL. Intraocular pressure fluctuation: a risk factor for visual field progression at low intraocular pressures in the advanced glaucoma intervention study. *Ophthalmology* 2008;115:1123–1129.
16. Lee J, Kim YK, Ha A, et al. Temporal raphe sign for discrimination of glaucoma from optic neuropathy in eyes with macular ganglion cell-inner plexiform layer thinning. *Ophthalmology* 2019;126:1131–1139.
17. Lee WJ, Kim YK, Park KH, Jeoung JW. Trend-based analysis of ganglion cell-inner plexiform layer thickness changes on optical coherence tomography in glaucoma progression. *Ophthalmology* 2017;124:1383–1391.
18. Kim SH, Park KH. The relationship between recurrent optic disc hemorrhage and glaucoma progression. *Ophthalmology* 2006;113:598–602.
19. Kwun Y, Lee EJ, Han JC, Kee C. Clinical characteristics of juvenile-onset open angle glaucoma. *Korean J Ophthalmol* 2016;30:127–133.
20. Hoesl LM, Mardin CY, Horn FK, Juenemann AG, Laemmer R. Influence of glaucomatous damage and optic disc size on glaucoma detection by scanning laser tomography. *J Glaucoma* 2009;18:385–389.
21. Suh MH, Kim DM, Kim YK, Kim TW, Park KH. Patterns of progression of localized retinal nerve fibre layer defect on red-free fundus photographs in normal-tension glaucoma. *Eye (Lond)* 2010;24:857–863.
22. Landis JR, Koch GG. The measurement of observer agreement for categorical data. *Biometrics* 1977;33:159–174.
23. Miki A, Medeiros FA, Weinreb RN, et al. Rates of retinal nerve fiber layer thinning in glaucoma suspect eyes. *Ophthalmology* 2014;121:1350–1358.
24. Lee EJ, Kim TW, Weinreb RN, Park KH, Kim SH, Kim DM. Trend-based analysis of retinal nerve fiber layer thickness measured by optical coherence tomography in eyes with localized nerve fiber layer defects. *Invest Ophthalmol Vis Sci* 2011;52:1138–1144.
25. Peng PH, Hsu SY, Wang WS, Ko ML. Age and axial length on peripapillary retinal nerve fiber layer thickness measured

by optical coherence tomography in nonglaucomatous Taiwanese participants. *PLoS One* 2017;12:e0179320.
26. Patel NB, Lim M, Gajjar A, Evans KB, Harwerth RS. Age-associated changes in the retinal nerve fiber layer and optic nerve head. *Invest Ophthalmol Vis Sci* 2014;55:5134–5143.
27. Parikh RS, Parikh SR, Sekhar GC, Prabakaran S, Babu JG, Thomas R. Normal age-related decay of retinal nerve fiber layer thickness. *Ophthalmology* 2007;114:921–926.
28. Morgan I, Rose K. How genetic is school myopia? *Prog Retin Eye Res* 2005;24:1–38.
29. Lee JH, Jee D, Kwon JW, Lee WK. Prevalence and risk factors for myopia in a rural Korean population. *Invest Ophthalmol Vis Sci* 2013;54:5466–5471.
30. Lin LL, Shih YF, Hsiao CK, Chen CJ. Prevalence of myopia in Taiwanese schoolchildren: 1983 to 2000. *Ann Acad Med Singap* 2004;33:27–33.
31. Chihara E, Liu X, Dong J, et al. Severe myopia as a risk factor for progressive visual field loss in primary open-angle glaucoma. *Ophthalmologica* 1997;211:66–71.
32. Perdicchi A, Iester M, Scuderi G, Amodeo S, Medori EM, Recupero SM. Visual field damage and progression in glaucomatous myopic eyes. *Eur J Ophthalmol* 2007;17:534–537.
33. Sohn SW, Song JS, Kee C. Influence of the extent of myopia on the progression of normal-tension glaucoma. *Am J Ophthalmol* 2010;149:831–838.
34. Han JC, Han SH, Park Y, Lee EJ, Kee C. Clinical course and risk factors for visual field progression in normal-tension glaucoma with myopia without glaucoma medications. *Am J Ophthalmol* 2020;209:77–87.
35. Bell GR. Biomechanical considerations of high myopia. Part I-Physiological characteristics. *J Am Optom Assoc* 1993;64:332–338.
36. Saw SM, Gazzard G, Shih-Yen EC, Chua WH. Myopia and associated pathological complications. *Ophthalmic Physiol Opt* 2005;25:381–391.
37. Read RM, Spaeth GL. The practical clinical appraisal of the optic disc in glaucoma: the natural history of cup progression and some specific disc-field correlations. *Trans Am Acad Ophthalmol Otolaryngol* 1974;78:255–274.
38. Sigal IA, Flanagan JG, Ethier CR. Factors influencing optic nerve head biomechanics. *Invest Ophthalmol Vis Sci* 2005;46:4189–4199.
39. Bellezza AJ, Hart RT, Burgoyne CF. The optic nerve head as a biomechanical structure: initial finite element modeling. *Invest Ophthalmol Vis Sci* 2000;41:2991–3000.
40. Kim YW, Jeoung JW, Kim DW, et al. Clinical assessment of lamina cribrosa curvature in eyes with primary open-angle glaucoma. *PLoS One* 2016;11:e0150260.
41. Kim YK, Yoo BW, Kim HC, Park KH. Automated detection of hemifield difference across horizontal raphe on ganglion cell–inner plexiform layer thickness map. *Ophthalmology* 2015;122:2252–2260.
42. Kim YK, Yoo BW, Jeoung JW, Kim HC, Kim HJ, Park KH. Glaucoma-diagnostic ability of ganglion cell-inner plexiform layer thickness difference across temporal raphe in highly myopic eyes. *Invest Ophthalmol Vis Sci* 2016;57:5856–5863.
43. Baek SU, Kim KE, Kim YK, Park KH, Jeoung JW. Development of topographic scoring system for identifying glaucoma in myopic eyes: a spectral-domain OCT study. *Ophthalmology* 2018;125:1710–1719.
44. Marshall HN, Andrew NH, Hassall M, et al. Macular ganglion cell-inner plexiform layer loss precedes peripapillary retinal nerve fiber layer loss in glaucoma with lower intraocular pressure. *Ophthalmology* 2019;126:1119–1130.
45. Gardiner SK, Johnson CA, Demirel S. Factors predicting the rate of functional progression in early and suspected glaucoma. *Invest Ophthalmol Vis Sci* 2012;53:3598–3604.
46. Gordon MO, Beiser JA, Brandt JD, et al. The Ocular Hypertension Treatment Study: baseline factors that predict the onset of primary open-angle glaucoma. *Arch Ophthalmol* 2002;120:714–720.
47. Kass MA, Heuer DK, Higginbotham EJ, et al. The Ocular Hypertension Treatment Study: a randomized trial determines that topical ocular hypotensive medication delays or prevents the onset of primary open-angle glaucoma. *Arch Ophthalmol* 2002;120:701–713.
48. Keltner JL, Johnson CA, Anderson DR, et al. The association between glaucomatous visual fields and optic nerve head features in the Ocular Hypertension Treatment Study. *Ophthalmology* 2006;113:1603–1612.
49. Drance S, Anderson DR, Schulzer M, for the Collaborative Normal-Tension Glaucoma Study Group. Risk factors for progression of visual field abnormalities in normal-tension glaucoma. *Am J Ophthalmol* 2001;131:699–708.
50. Prum BE Jr, Lim MC, Mansberger SL, et al. Primary open-angle glaucoma suspect preferred practice pattern guidelines. *Ophthalmology* 2016;123:112–151.
51. Chang RT, Singh K. Glaucoma suspect: diagnosis and management. *Asia Pac J Ophthalmol* 2016;5:32–37.
52. Quigley HA, Katz J, Derick RJ, Gilbert D, Sommer A. An evaluation of optic disc and nerve fiber layer examinations in monitoring progression of early glaucoma damage. *Ophthalmology* 1992;99:19–28.
53. Xu G, Weinreb RN, Leung CK. Optic nerve head deformation in glaucoma: the temporal relationship between optic nerve head surface depression and retinal nerve fiber layer thinning. *Ophthalmology* 2014;121:2362–2370.
54. Budenz DL, Anderson DR, Feuer WJ, et al. Detection and prognostic significance of optic disc hemorrhages during the Ocular Hypertension Treatment study. *Ophthalmology* 2006;113:2137–2143.
55. Yamamoto T, Iwase A, Kawase K, Sawada A, Ishida K. Optic disc hemorrhages detected in a large-scale eye disease screening project. *J Glaucoma* 2004;13:356–360.
56. Kim DW, Kim YK, Jeoung JW, Kim DM, Park KH. Prevalence of optic disc hemorrhage in Korea: the Korea National Health and Nutrition Examination Survey. *Invest Ophthalmol Vis Sci* 2015;56:3666–3672.
57. Leung CK, Chiu V, Weinreb RN, et al. Evaluation of retinal nerve fiber layer progression in glaucoma: a comparison between spectral-domain and time-domain optical coherence tomography. *Ophthalmology* 2011;118:1558–1562.
58. Wang X, Li S, Fu J, et al. Comparative study of retinal nerve fibre layer measurement by RTVue OCT and GDx VCC. *Br J Ophthalmol* 2011;95:509–513.